SUPPORTING INFORMATION

Probing the Association of Frustrated Phosphine-Borane Lewis Pairs in Solution by NMR Spectroscopy

Luca Rocchigiani,[†,*] *Gianluca Ciancaleoni,*[‡] *Cristiano Zuccaccia,*[†] *and Alceo Macchioni,*[†,*]

[†]Dipartimento di Chimica, Biologia e Biotecnologie - Università degli Studi di Perugia, Via Elce di Sotto, 8, I-06123, Perugia (Italy) Fax: (+)39 075 5855598
E-mail: luca.rocchigiani@progetti.unipg.it
alceo.macchioni@unipg.it

[‡]Istituto del CNR di Scienze e Tecnologie Molecolari (CNR-ISTM) c/o Dipartimento di Chimica Università degli Studi di Perugia, I-06123, Perugia (Italy)

1. Experimental details

All manipulations were performed in flamed Schlenk glassware on a Schlenk line interfaced to a high-vacuum pump (10^{-5} mmHg) or in a nitrogen-filled VAC glovebox with a high capacity recirculator (< 1 ppm of O_2 and H2O). toluene-d_8 and benzene-d_6 (Cortecnet) were freeze-pump-thaw degassed over Na/K alloy, and vacuum-transferred into a storage Schlenk with a PTFE valve. C_6F_6 (Carlo Erba) was freeze-pump-thaw degassed over CaH_2 and vacuum transferred into a storage Schlenk with a PTFE valve. Tri-*tert*-butylphosphine was purchased from Sigma-Aldrich and used as received; trimesitylphosphine was purchased from Sigma Aldrich and vacuum dried before using. $B(C_6F_5)_3$ was obtained from Boulder Scientific and purified by vacuum sublimation. 1D- and 2D-NMR spectra were measured on a Bruker DRX Avance 400 spectrometer equipped with a QNP probe or an a Bruker Avance III HD 400 spectrometer equipped with a smartprobe. Referencing is relative to residual of undeuterated solvents (^{1}H), CCl_3F (^{19}F) and 85% H_3PO_4 (^{31}P).

In the case of $P(t\text{-}bu)_3$ / $B(C_6F_5)_3$ mixtures, NMR spectra were recorded at 265 K in order to avoid decomposition. $P(Mes)_3$ / $B(C_6F_5)_3$ mixtures showed no signs of decomposition over the period of several weeks, even if the color of the solution turns from light pink to orange independently of the used solvent.

NMR data of stoichiometric mixtures

$P(t\text{-}bu)_3$ + $B(C_6F_5)_3$ ^{1}H NMR (400.13 MHz, toluene-d_8, 265 K) δ 1.25 ppm (d, $J_{H,P}$= 9.7 Hz, t-bu). ^{19}F NMR (376.5 MHz, toluene-d_8, 265 K) δ –129.2 (brd, 2F, *ortho*-F), –142.0 (brd, 1F, *para*-F), –160.6 ppm (brd, 2F, *meta*-F). ^{31}P{^{1}H} NMR (150.0 MHz, toluene-d_8, 265 K) δ 61.2 ppm (s, $P(t\text{-}bu)_3$).

$P(Mes)_3$ + $B(C_6F_5)_3$ ^{1}H NMR (400.13 MHz, toluene-d_8, 298 K) δ 6.70 (brd, 2H, *meta*-H), 2.19 (brd, 6H, *ortho*-CH_3), 2.10 (s, 3H, *para*-CH_3). ^{19}F NMR (376.5 MHz, toluene-d_8, 298 K) δ –129.2 (d, 2F, $^3J_{F,F}$=20.2 Hz, *ortho*-F), –142.7 (brd, 1F, *para*-F), –160.7 ppm (m, 2F, *meta*-F). ^{31}P{^{1}H} NMR (150.0 MHz, toluene-d_8, 298 K) δ –35.4 ppm (s, $P(Mes)_3$).

$P(Mes)_3$ + C_6F_6 ^{1}H NMR (400.13 MHz, benzene-d_6, 298 K) δ 6.73 (brd, 2H, *meta*-H), 2.23 (brd, 6H, *ortho*-CH_3), 2.10 (s, 3H, *para*-CH_3). ^{19}F NMR (376.5 MHz, benzene-d_6, 298 K) δ -163.2 ppm (s, C_6F_6). ^{31}P{^{1}H} NMR (150.0 MHz, benzene-d_6, 298 K) δ –35.1 ppm (s, $P(Mes)_3$).

2. ^{19}F, ^{1}H HOESY NMR experiments

Quantitative and semi-quantitative two-dimensional ^{19}F, ^{1}H HOESY NMR spectra were measured by using the standard four pulses sequence (phase sensitive version).[1] The number of transients and data points were chosed according to the sample concentration and the desided final digital resolution. Semiquantitative spectra were recorded using a 1 s relaxation delay and 800 ms mixing time. Quantitative experiments were obtained for $P(Mes)_3/B(C_6F_5)_3$ mixtures using a 7.5 s relaxation delay and 200 ms mixing time, once having determined the T_1 values for both ^{1}H and ^{19}F signals (see below).

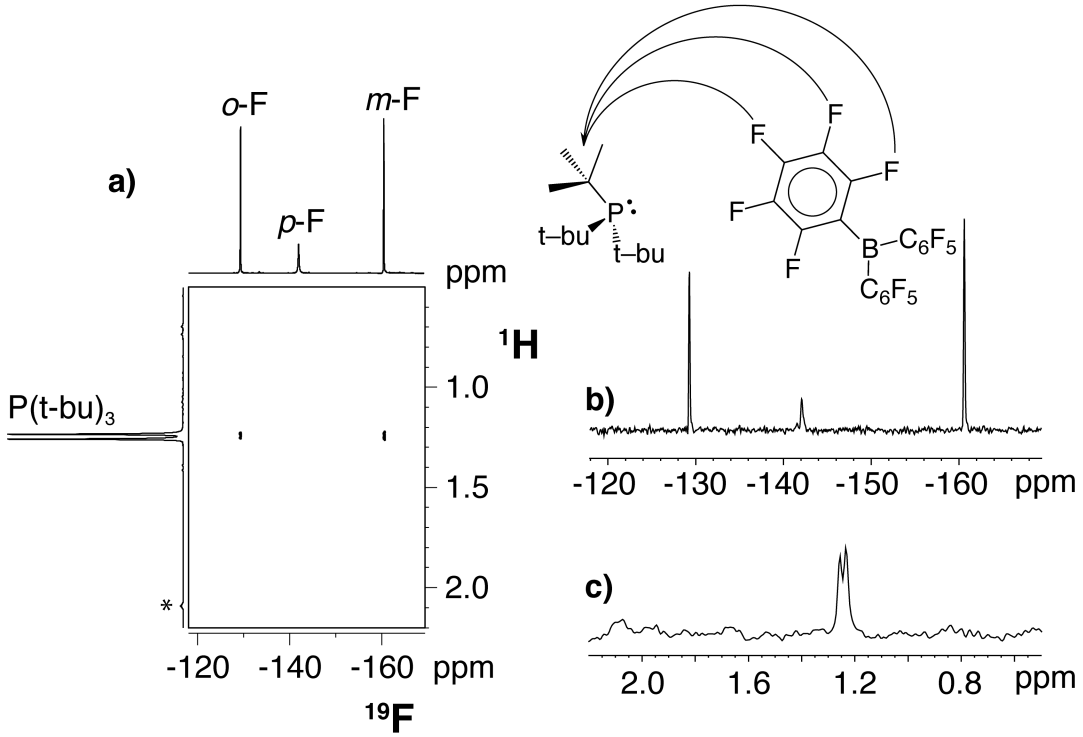

Figure S1. a) ^{19}F, ^{1}H HOESY NMR spectrum of $P(t\text{-bu})_3/B(C_6F_5)_3$ (C=225 mM, T=265K, solvent=toluene-d_8, relaxation delay=1 s, mixing time=800 ms); b) F2 trace at δ_H=1.25 ppm; c) F1 trace at δ_F=–160.5 ppm. Asterisk denotes residual solvent.

(1) Lix, B.; Sönnichsen, F.D.; Sykes, B.D. *J. Magn. Reson. Ser. A* **1996**, *121*, 83.

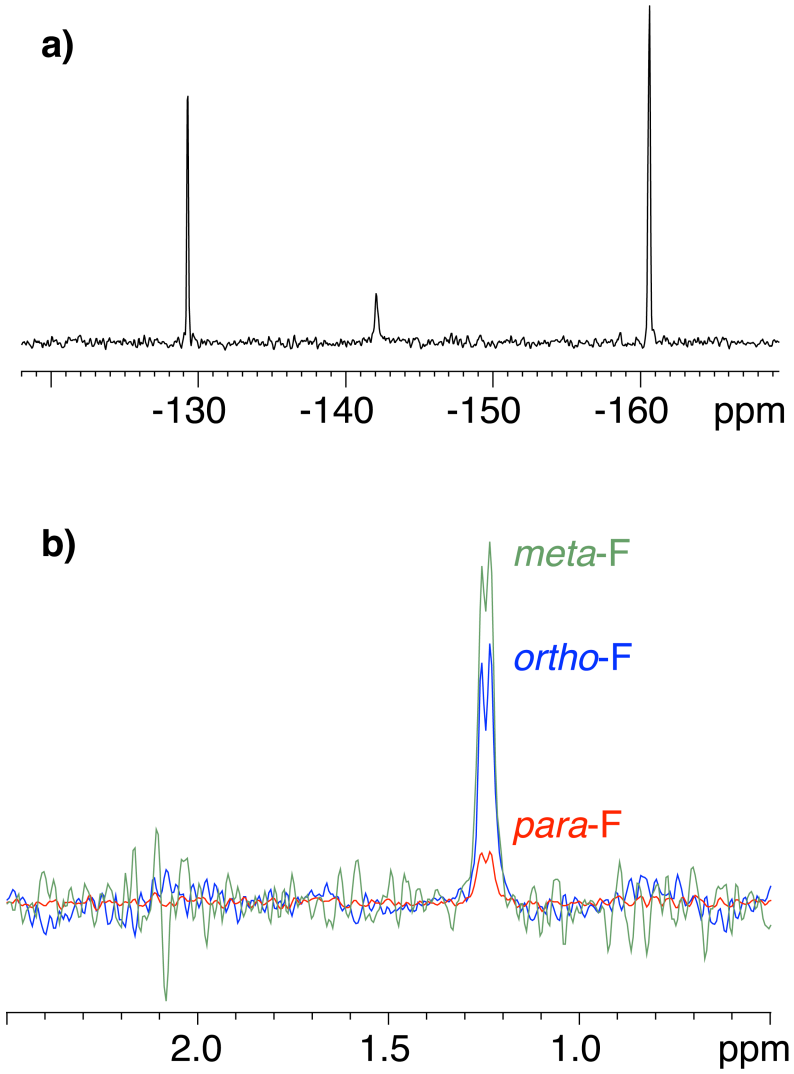

Figure S2. a) F2 trace and b) F1 traces extracted from the ^{19}F, ^{1}H HOESY NMR spectrum of a P(t-bu)$_3$ and B(C_6F_5)$_3$ 1:1 mixture (C=225 mM, T=265K, solvent=toluene-d_8, relaxation delay = 1 s, mixing time = 800 ms).

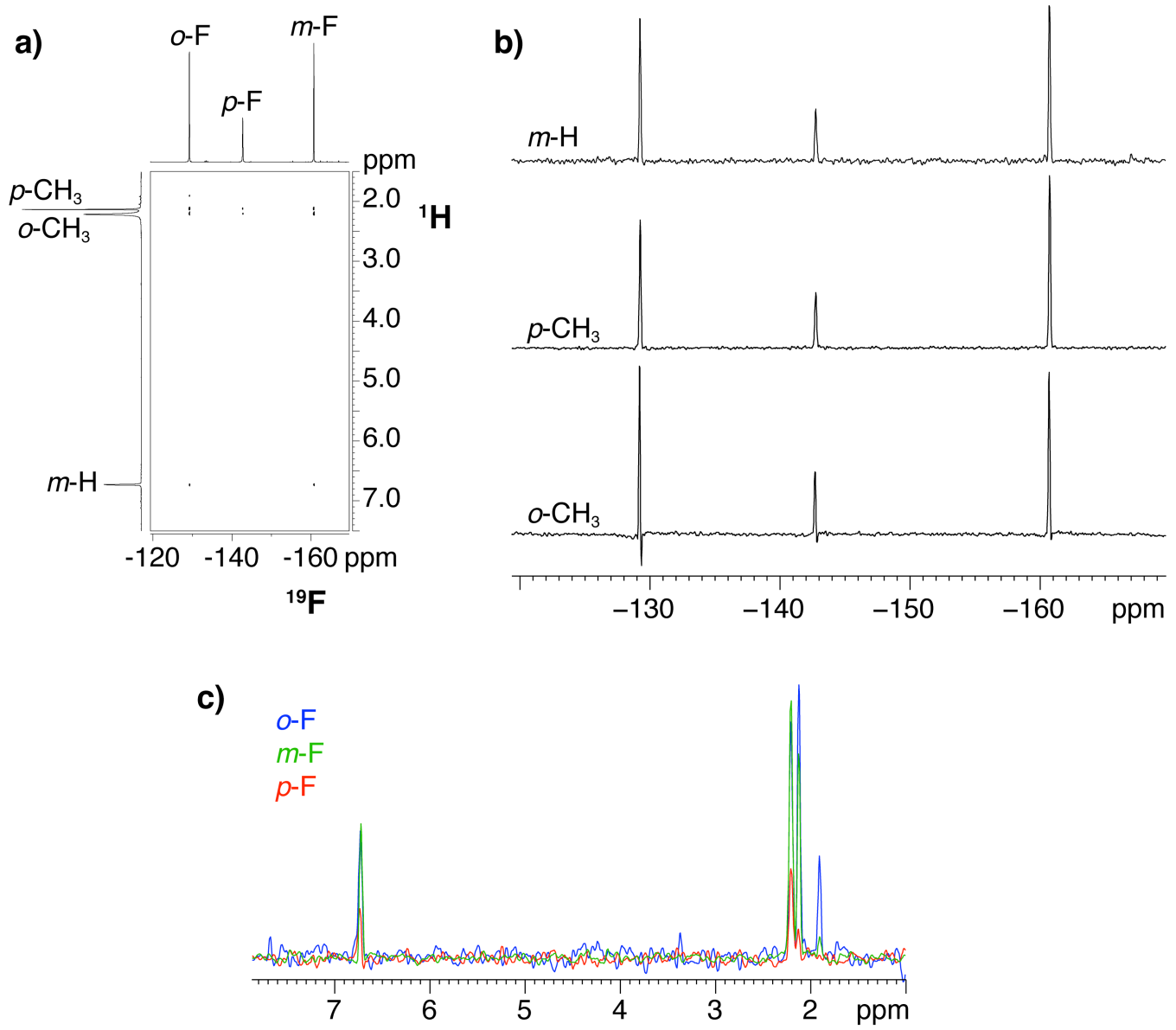

Figure S3. a) ^{19}F, ^{1}H HOESY NMR spectrum of a $P(Mes)_3$ / $B(C_6F_5)_3$ 1:1 mixture (C= 250 mM, T=298K, solvent=toluene-d_8, relaxation delay 1 s, mixing time=800 ms; b) F1 and c) F2 traces exctracted from 2D spectrum.

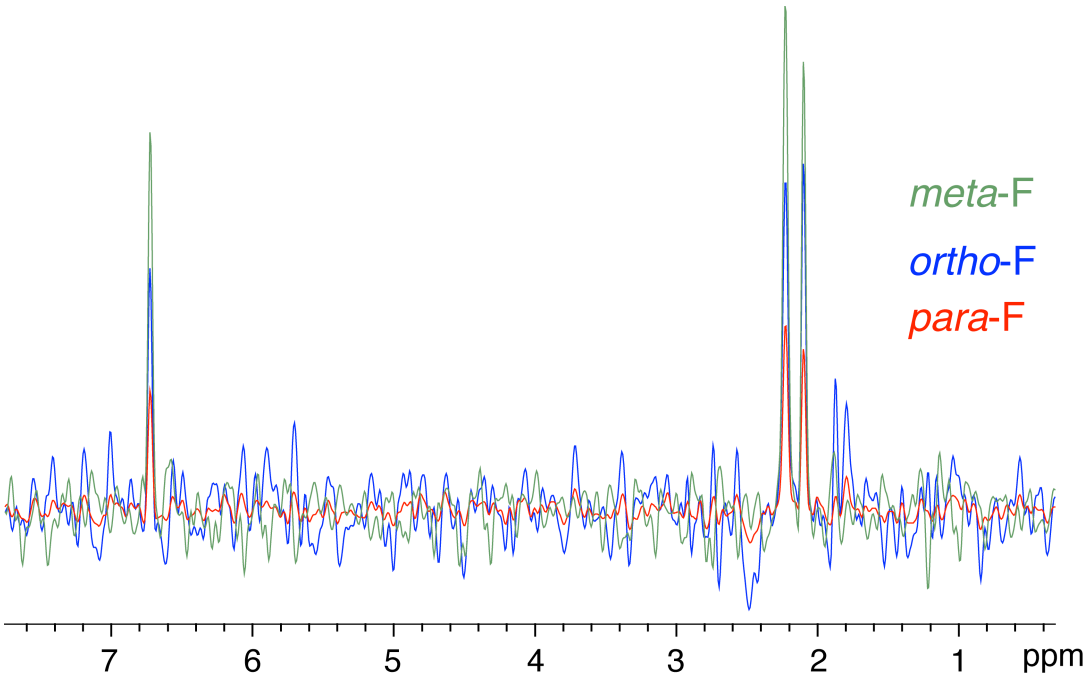

Figure S4. F2 traces extracted from the ^{19}F, ^{1}H HOESY NMR spectrum of a $P(Mes)_3$ / $B(C_6F_5)_3$ 1:1 mixture (C=228 mM, T=298K, solvent=benzene-d_6, relaxation delay = 7.5 s, mixing time = 200 ms).

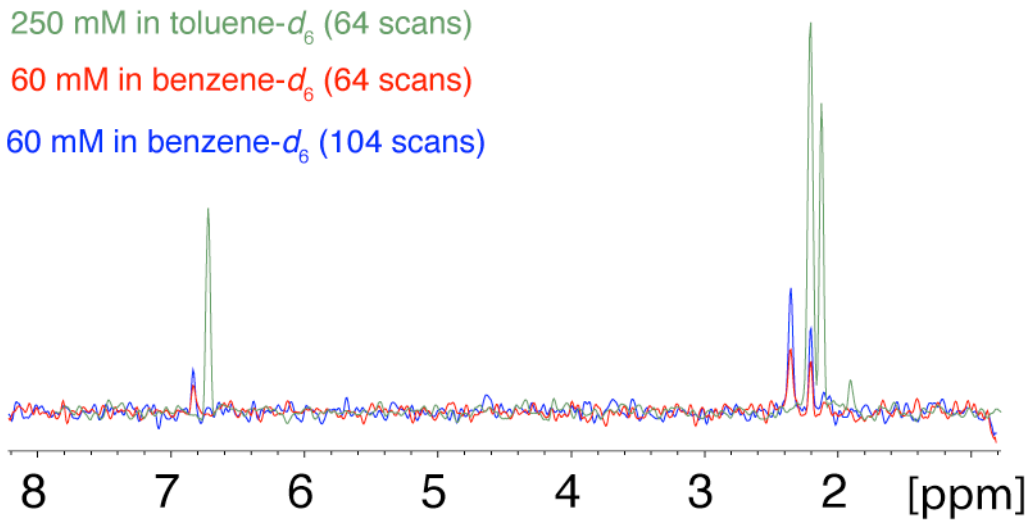

Figure S5. F2 traces extracted for *m*-F resonance in three different ^{19}F, ^{1}H HOESY experiments of a 1:1 $P(Mes)_3$ / $B(C_6F_5)_3$ mixture (60 mM acquired with 64 scans, red trace; 60 mM acquired with 104 scans, blue trace, 250 mM acquired with 64 scans, green trace).

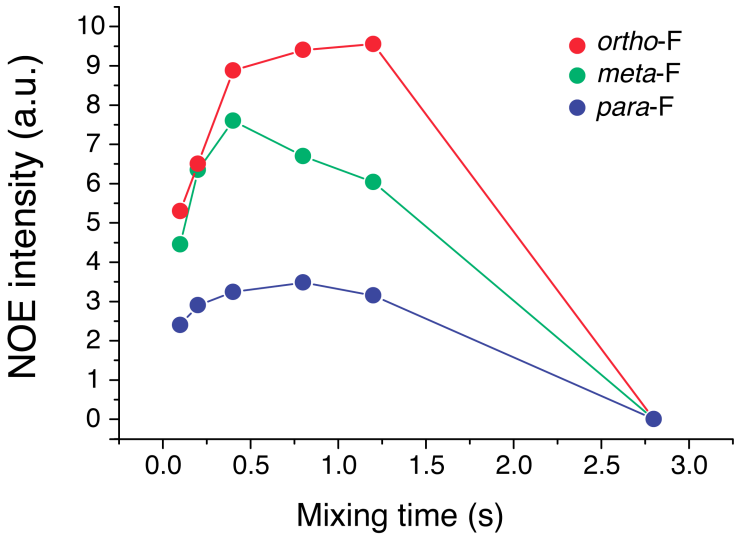

Figure S6. Evolution of NOE intensity due to *ortho*-CH_3 signal (integral of 2D peak) as a function of mixing time measured for a 1:1 $P(Mes)_3$ / $B(C_6F_5)_3$ in benzene-d_6 by means of ^{19}F, ^{1}H HOESY NMR experiments.

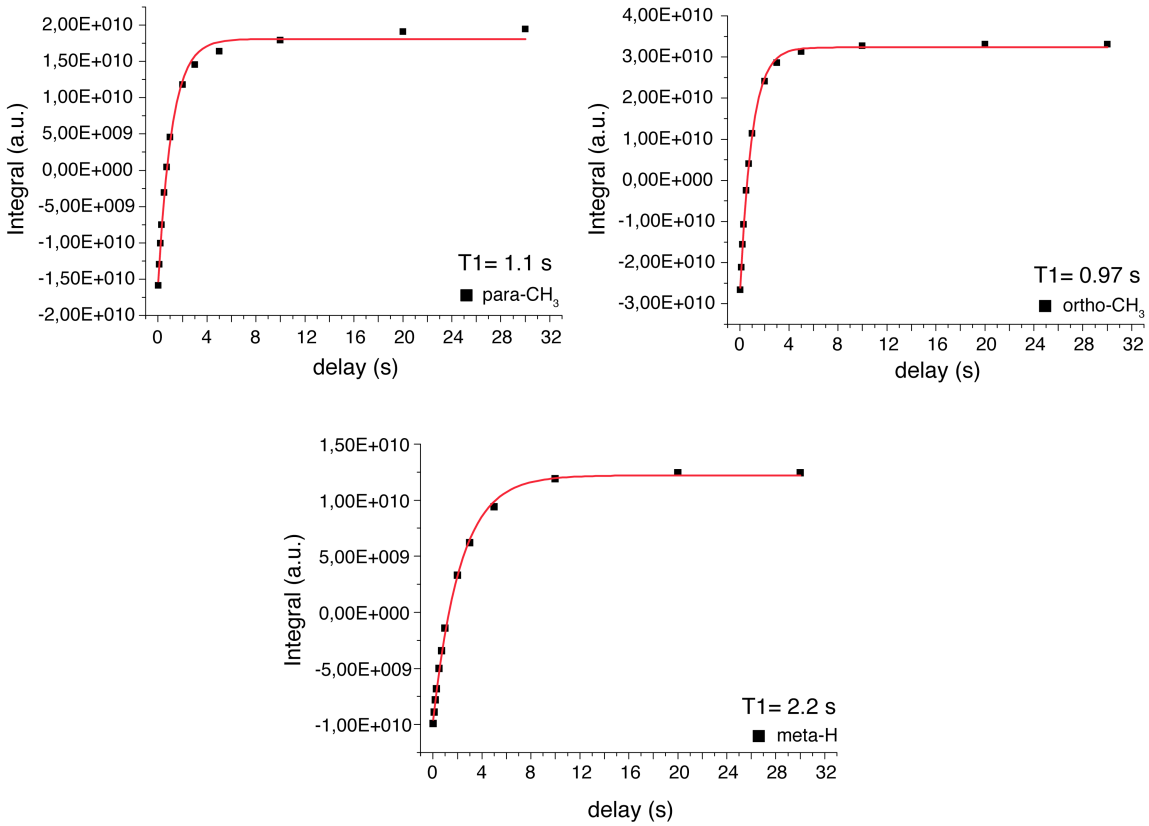

Figure S7. ^{1}H T1 measurements of a 1:1 $P(Mes)_3$ / $B(C_6F_5)_3$ mixture in toluene-d_8 at 298K (C=250 mM).

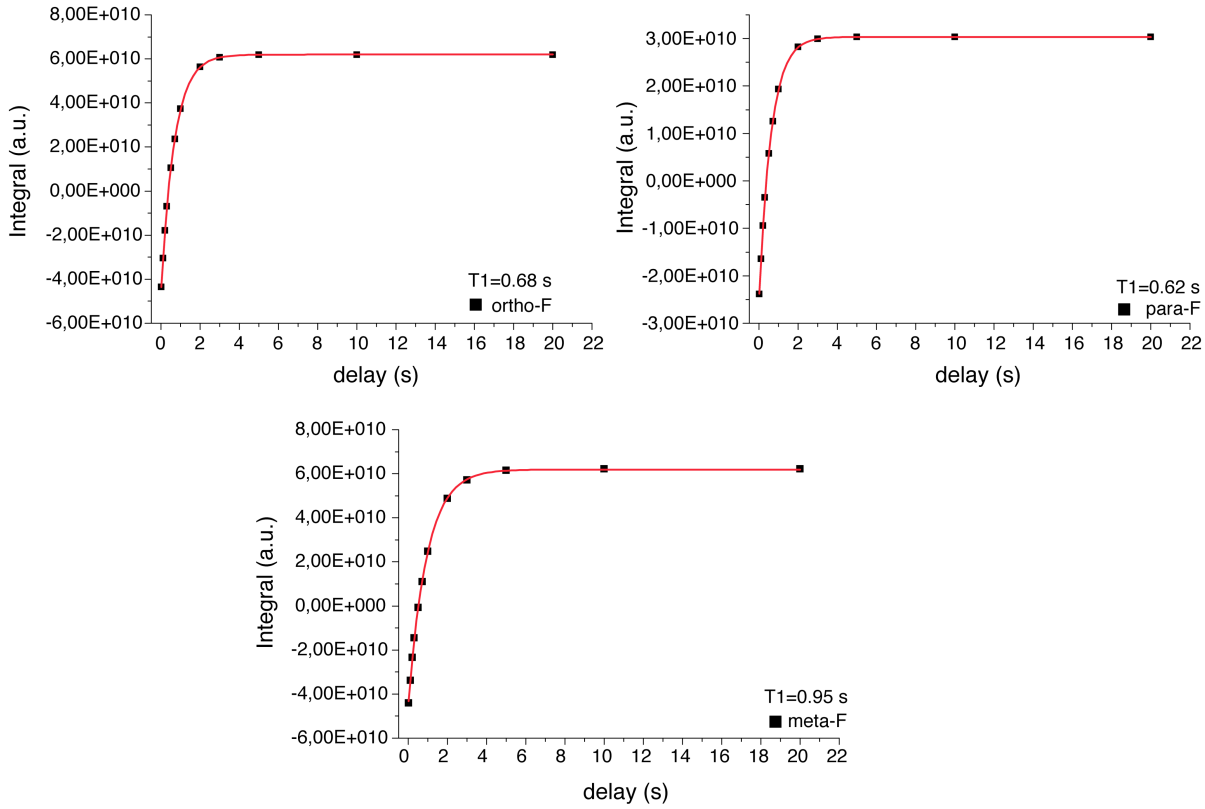

Figure S8. ^{19}F T1 measurements of a 1:1 $P(Mes)_3$ / $B(C_6F_5)_3$ mixture in toluene-d_8 at 298K (C=250 mM).

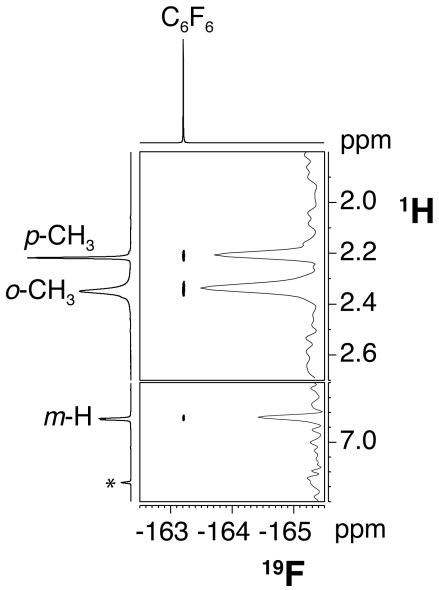

Figure S9. ^{19}F, ^{1}H HOESY NMR spectrum of a $P(Mes)_3/C_6F_6$ 1:1 mixture (C=270 mM, T=298K, solvent=benzene-d_6, relaxation delay=1 s, mixing time=800 ms); the corresponding F2 trace is reported inside the 2D spectrum. Asterisk denote undeuterated solvent.

2. VT NMR Spectra

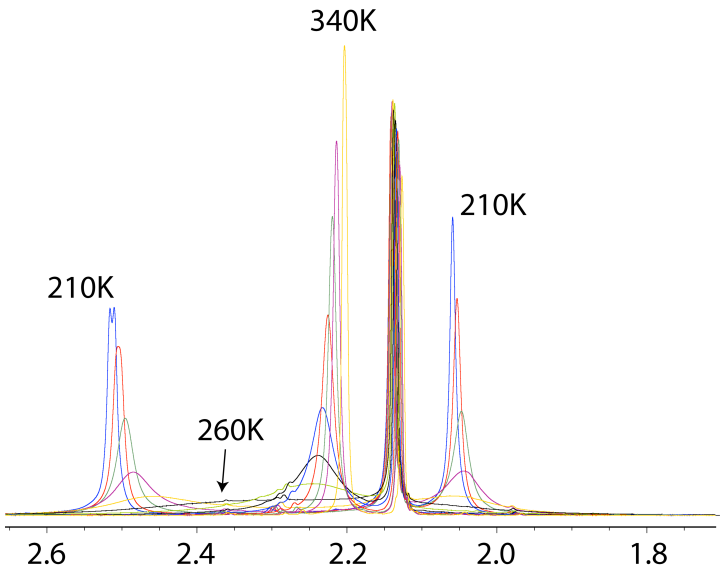

Figure S10. VT ^{1}H NMR spectra (210-340K temperature range) of a sample of $PMes_3$ (C=240 mM) in toluene-d_8 showing the coalescence of the *ortho*-CH_3 resonances due to the hindered rotation of the mesityl ring on the P–C bond.

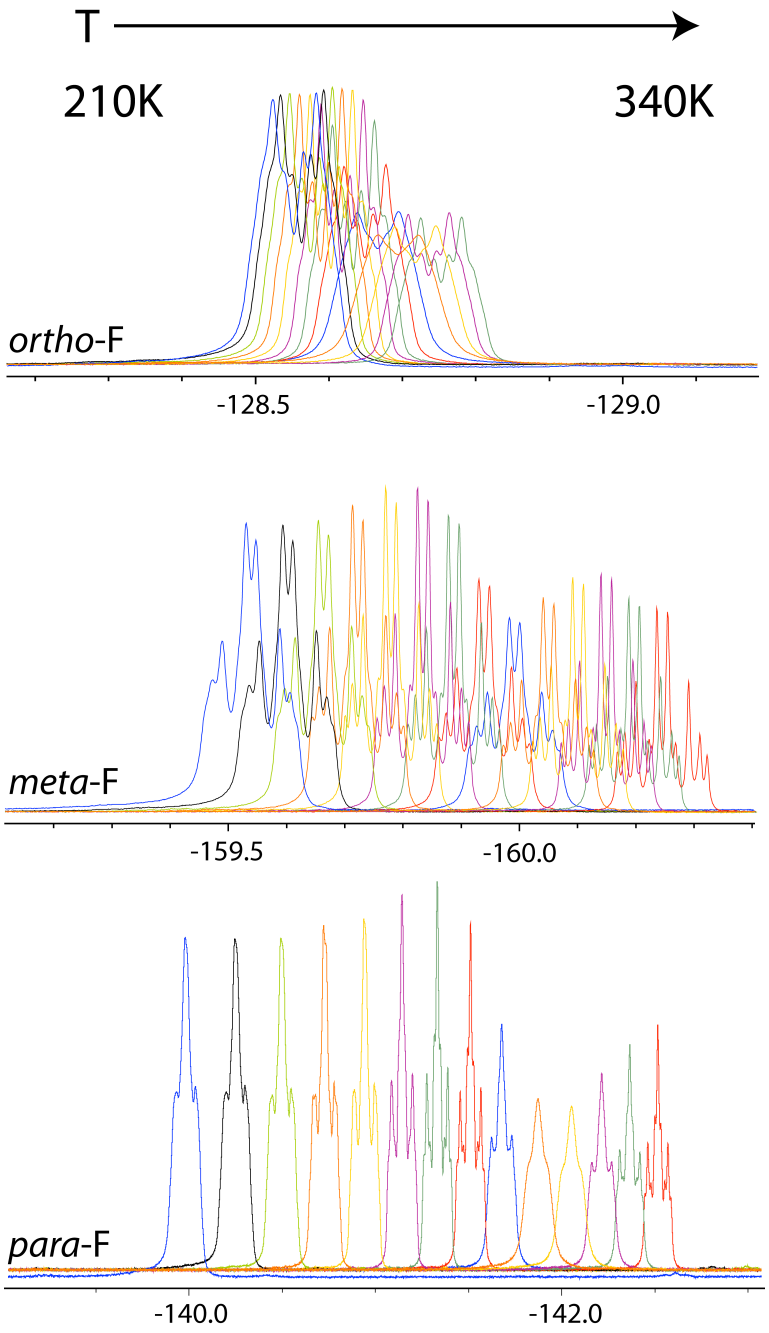

Figure S11. VT ^{19}F NMR spectra (210-340K temperature range) of a sample of $B(C_6F_5)_3$ (C=15 mM) in toluene-d_8 showing the substantial independence of line broadening with the temperature.

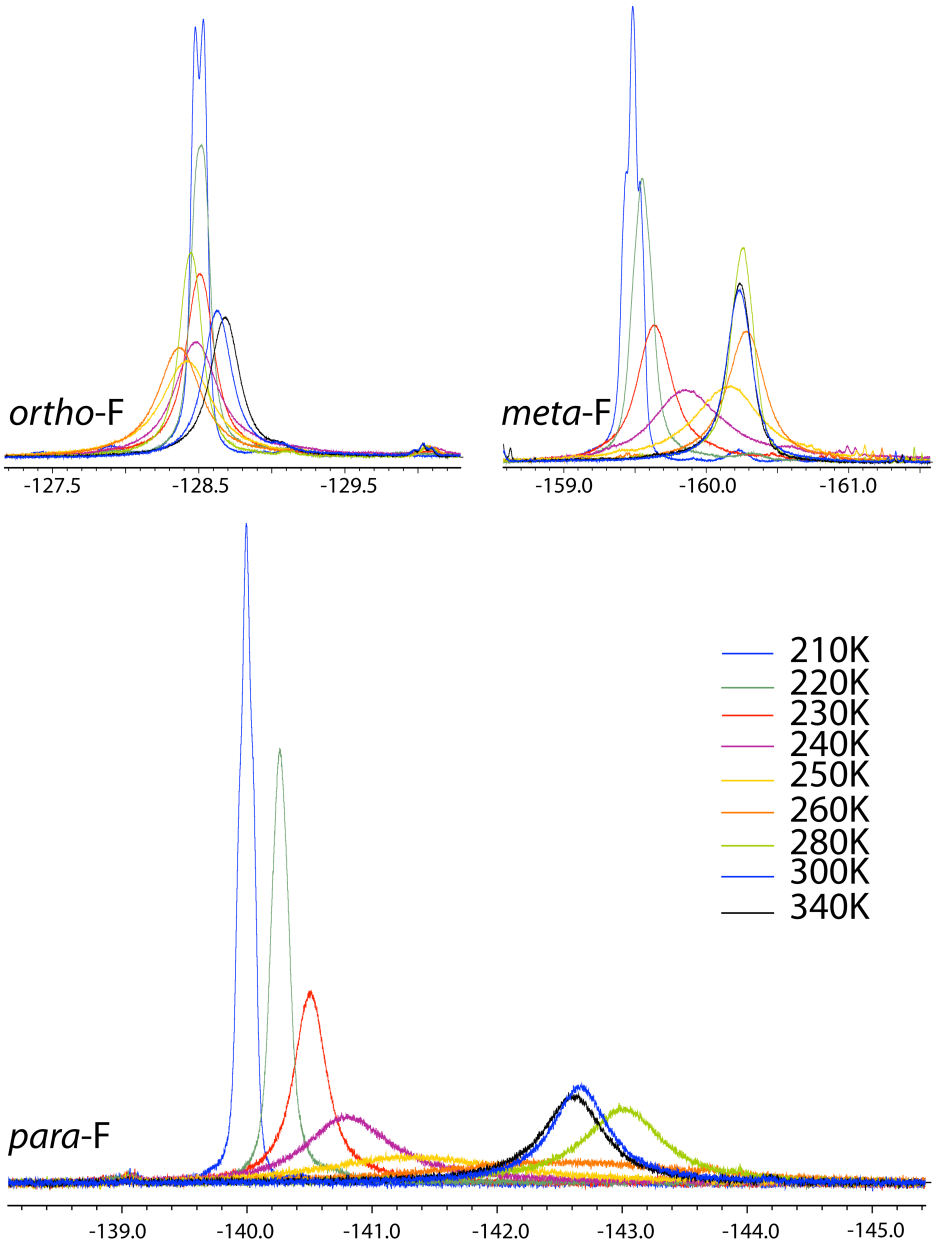

Figure S12. VT ^{19}F NMR spectra (210-340K temperature range) of a sample containing $B(C_6F_5)_3$ (C=15 mM) and $PMes_3$ (C=240mM) in toluene-d_8.

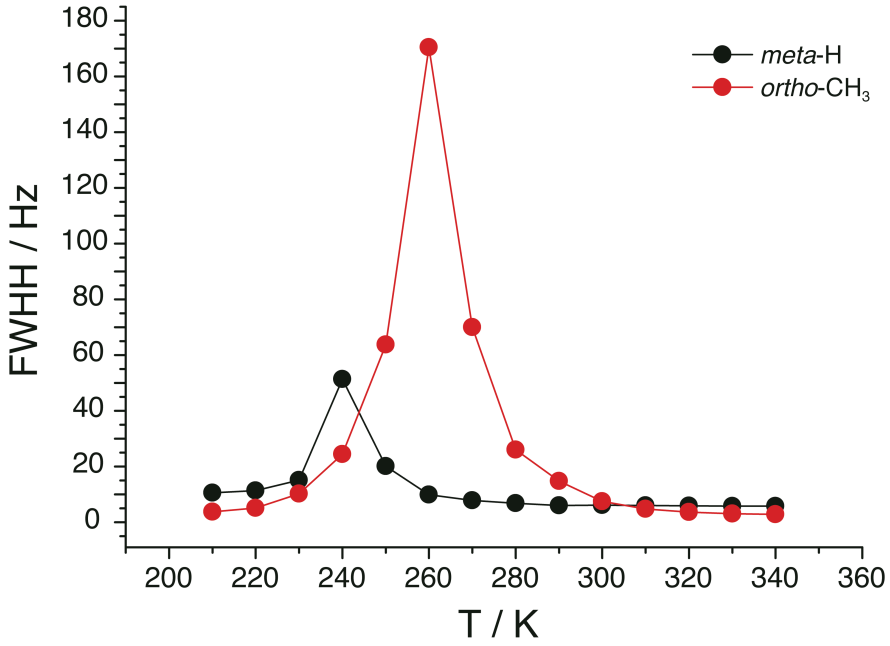

Figure S13. Evolution of the full width at half height as a function of the temperature of the signals due *meta*-H and *ortho*-CH_3 of a sample containing $PMes_3$ (240 mM) and $B(C_6F_5)_3$ (15 mM) in toluene-d_8.

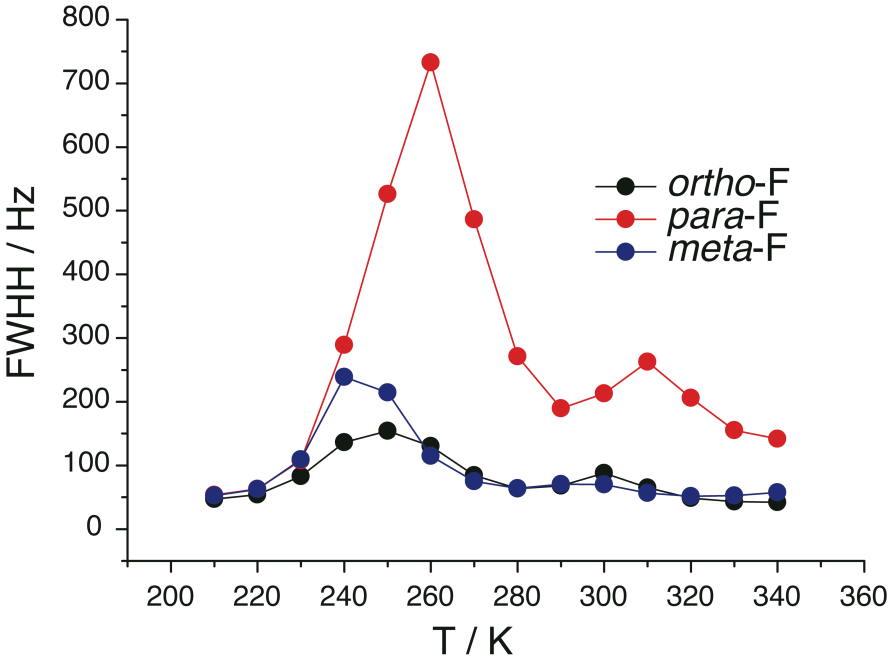

Figure S14. Evolution of the full width at half height as a function of the temperature of the signals due *ortho*-, *meta- and para*-F of a sample containing $PMes_3$ (240 mM) and $B(C_6F_5)_3$ (15 mM) in toluene-d_8.

4. PGSE NMR experiments

^{1}H and ^{19}F PGSE NMR measurements were performed by using the standard stimulated echo sequence (or the double stimulated echo version with longitudinal eddy current delay) on a Bruker DRX Avance 400 spectrometer equipped with a QNP probe or an a Bruker Avance III HD 400 spectrometer equipped with a smartprobe with the Z-gradient coil at 298K without spinning. The dependence of the resonance intensity (I) on a constant waiting time and on a varied gradient strenght G is described by the following equation:

$$\ln\frac{I}{I_0} = (\gamma\delta)^2 D_t\left(\Delta - \frac{\delta}{3}\right)G^2$$

where I is the intensity of the observed spin echo, I_0 the intensity of the spin echo in the absence of gradient, D_t the self-diffusion coefficient, Δ the delay between the midpoints of the gradients, δ the length of the gradient pulse, and γ the magnetogyric ratio. The shape of the gradients was rectangular, their length δ was 4–5 ms, and their strength G was varied during the experiments. All spectra were acquired for 32k points and a spectral width of 5000 (1H) and 18000 (19F) and processed with a line broadening of 1.0. The semi-logarithmic plots of $\ln(I/I_0)$ versus G^2 were fitted by using a standard linear regression algorithm, and a correlation factor better than 0.99 was always obtained. Different values of Δ, G, and number of transients were used for different samples.

The self-diffusion coefficient D_t, which is directly proportional to the slope *m* of the regression line obtained by plotting $\ln(I/I_0)$ versus G^2, was estimated by evaluating the proportionality constant for a sample of HDO (5%) in D_2O (known diffusion coefficients in the range 274–318 K)[2] under the exact same conditions as the sample of interest. The solvent was taken as internal standard. The D_t data were treated as described in the literature in order to derive the hydrodymanic dimensions.[3] The measure- ment uncertainty was estimated by determining the standard deviation of *m* when performing experiments with different Δ values. Error propagation analysis yielded a standard deviation of approximately 3–4 % in the hydrodynamic radius.

(2) (a) Tyrrell, H.J.W.; Harris, K.R. Diffusion in Liquids; Butterworth: London, **1984**. (b) Mills, R. *J. Phys. Chem.* **1973**, *77*, 685.
(3) Macchioni, A.; Ciancaleoni, G.; Zuccaccia, C.; Zuccaccia, D. *Chem. Soc. Rev.* **2008**, *37*, 479.

PGSE data

Linear fittings of $\ln(I/I_0)$ versus G^2 for ^1H and ^{19}F PGSE NMR experiments (298 K) are reported below.

Sample 1 - C $PMes_3$=3.1 mM
C $B(C_6F_5)_3$ =463.0 mM

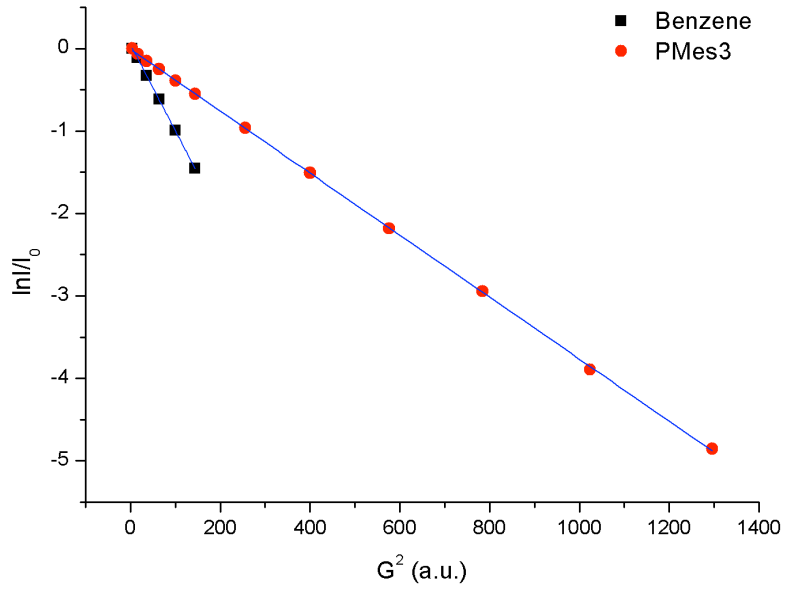

Figure S15. Log(I/I_0) versus G^2 of $PMes_3$ (3.1 mM) + $B(C_6F_5)_3$ (463.0 mM) in benzene-d_6.

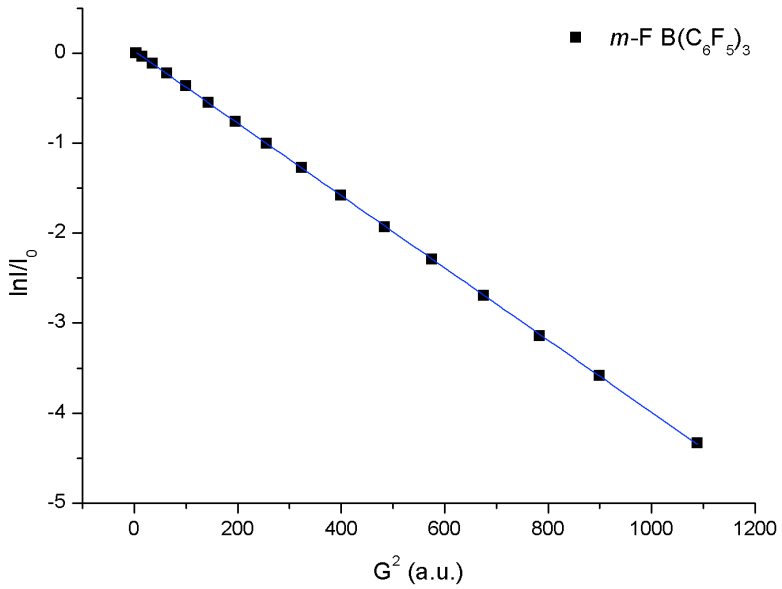

Figure S16. Log(I/I_0) versus G^2 of $PMes_3$ (3.1 mM) + $B(C_6F_5)_3$ (463.0 mM) in benzene-d_6.

Sample 2 - C $PMes_3$=4.5 mM
C $B(C_6F_5)_3$ =357.5 mM

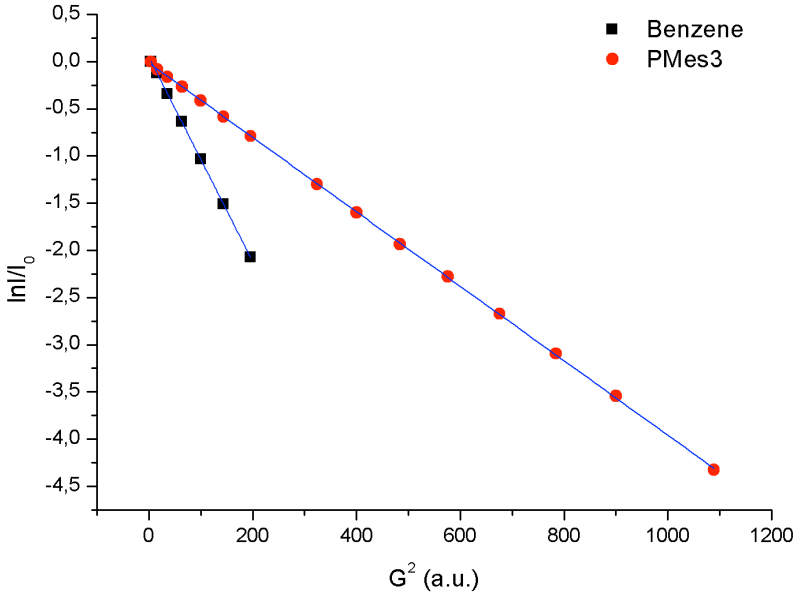

Figure S17. Log(I/I_0) versus G^2 of $PMes_3$ (4.5 mM) + $B(C_6F_5)_3$ (357.5 mM) in benzene-d_6.

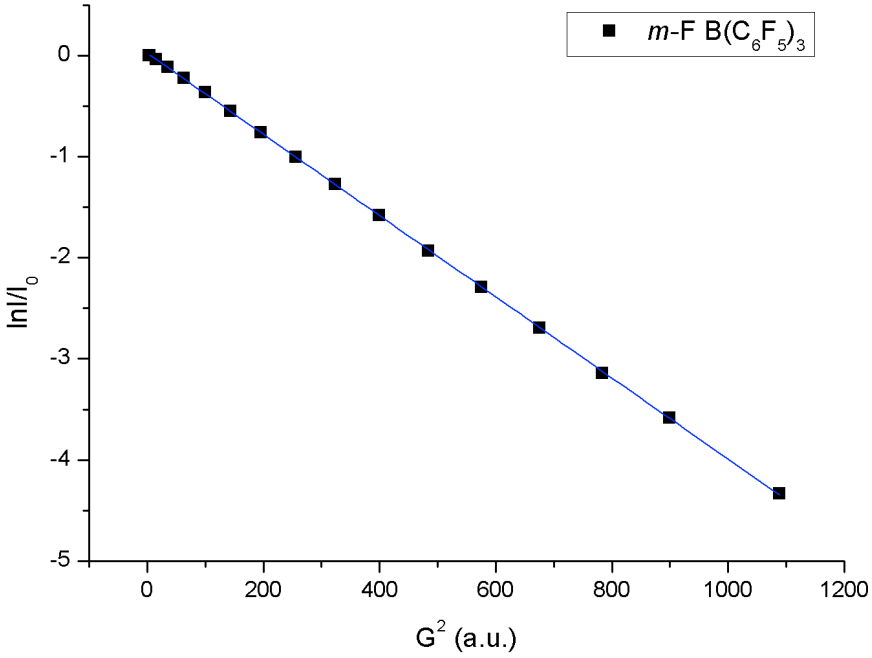

Figure S18. Log(I/I_0) versus G^2 of $PMes_3$ (4.5 mM) + $B(C_6F_5)_3$ (357.5 mM) in benzene-d_6.

Sample 3 - C $PMes_3$=5.8 mM
C $B(C_6F_5)_3$ =251.6 mM

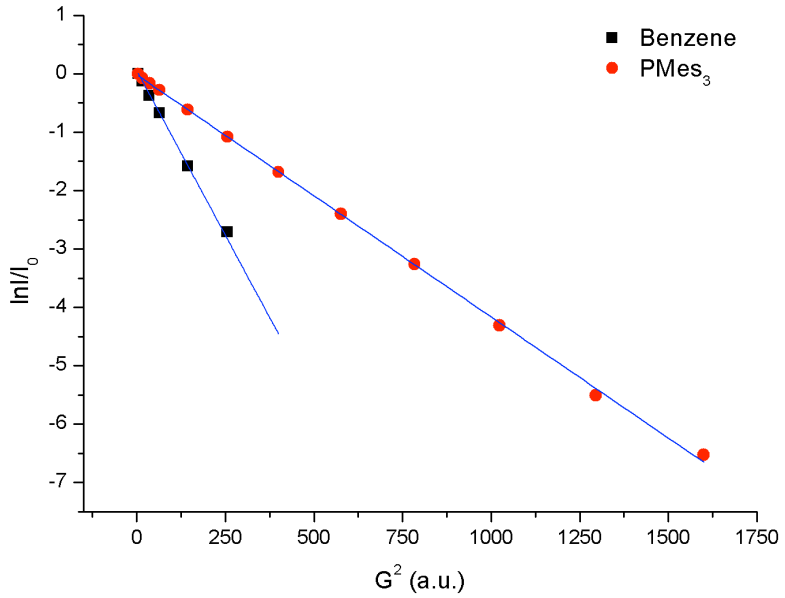

Figure S19. Log(I/I_0) versus G^2 of $PMes_3$ (5.8 mM) + $B(C_6F_5)_3$ (251.6 mM) in benzene-d_6.

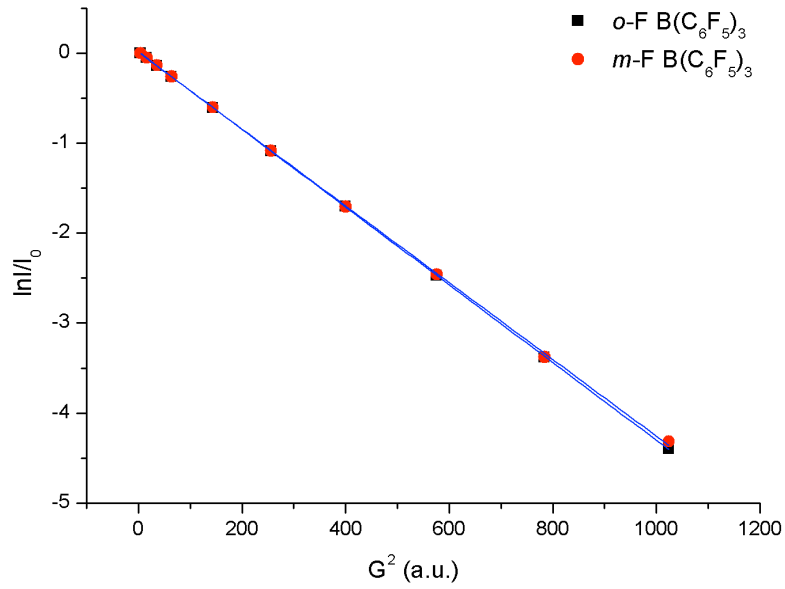

Figure S20. Log(I/I_0) versus G^2 of $PMes_3$ (5.8 mM) + $B(C_6F_5)_3$ (251.6 mM) in benzene-d_6.

Sample 4 - C $PMes_3$=38.7 mM
C $B(C_6F_5)_3$ =463.0 mM

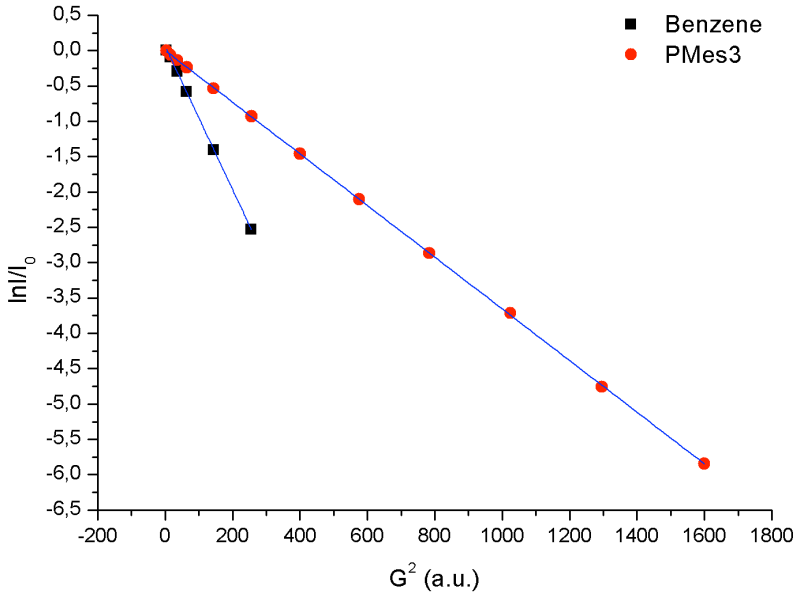

Figure S21. Log(I/I_0) versus G^2 of $PMes_3$ (38.7 mM) + $B(C_6F_5)_3$ (463.0 mM) in benzene-d_6.

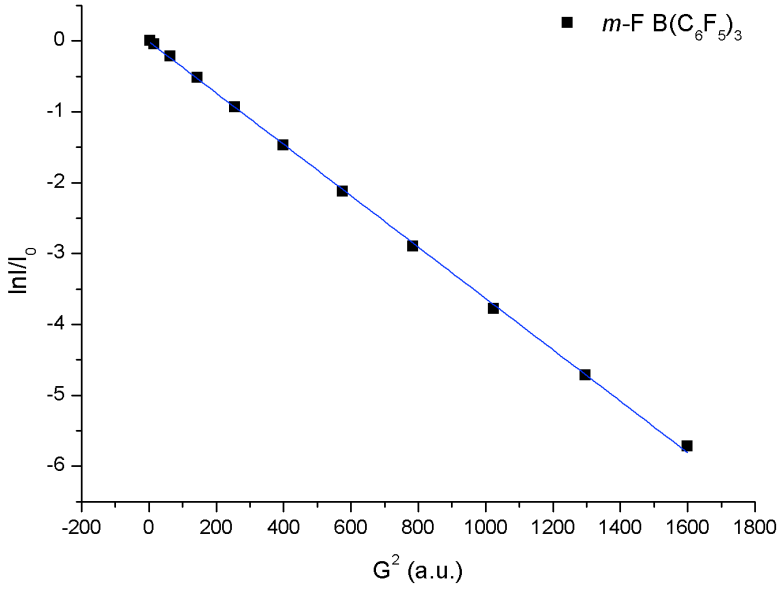

Figure S22. Log(I/I_0) versus G^2 of $PMes_3$ (38.7 mM) + $B(C_6F_5)_3$ (463.0 mM) in benzene-d_6.

Sample 5 - C $PMes_3$=345.7 mM
C $B(C_6F_5)_3$ =40.7 mM

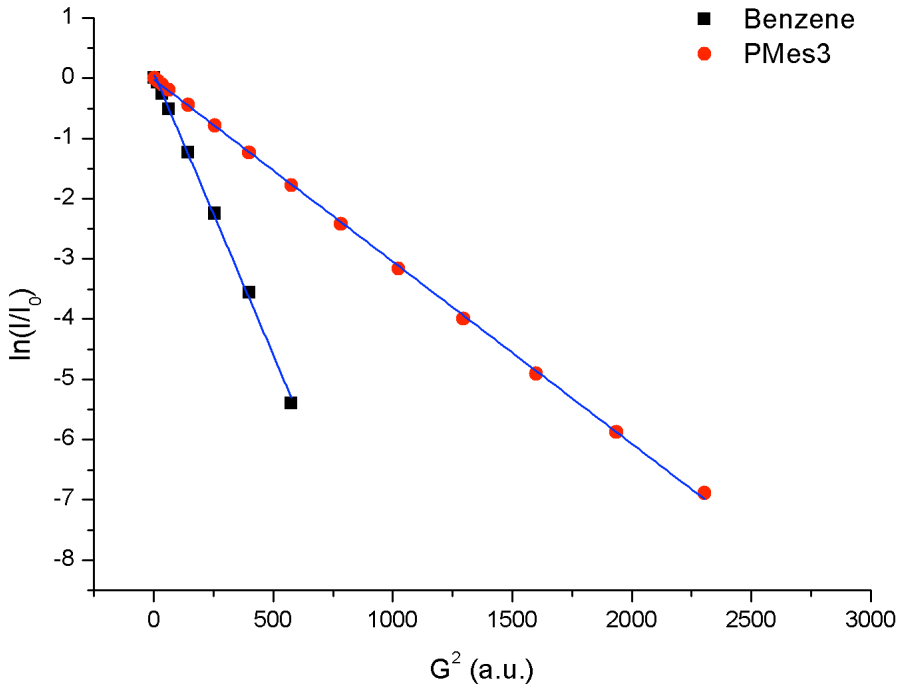

Figure S23. Log(I/I_0) versus G^2 of $PMes_3$ (345.7 mM) + $B(C_6F_5)_3$ (40.7 mM) in benzene-d_6.

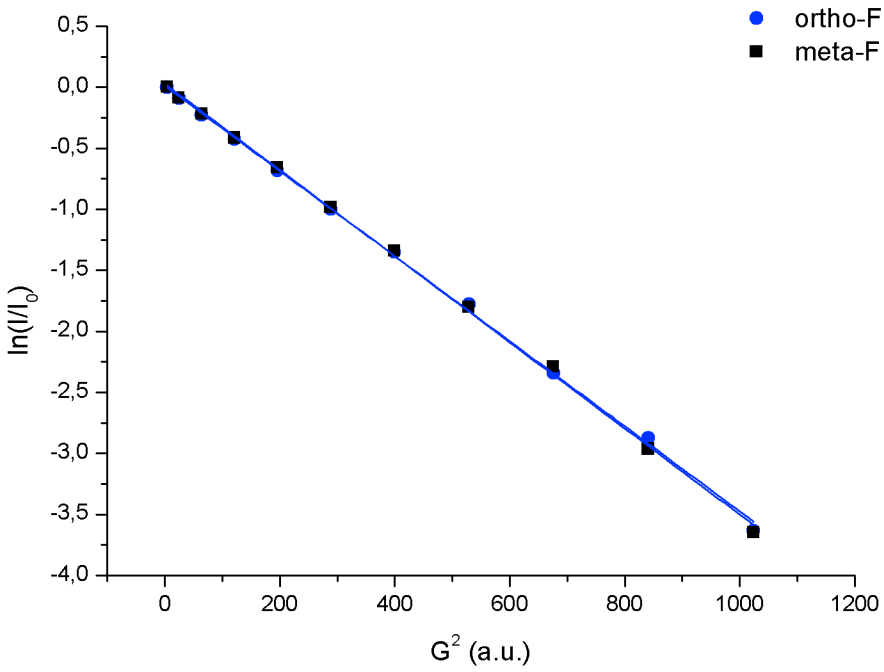

Figure S24. Log(I/I_0) versus G^2 of $PMes_3$ (345.7 mM) + $B(C_6F_5)_3$ (40.7 mM) in benzene-d_6.

6. DFT Calculations

Computational Details. All calculations reported in this work have been performed using density functional theory (DFT) with the ADF (Amsterdam Density functional) package.[4] The BP86 GGA functional was used.[5] The dispersion corrections were taken into account using the Grimme D3-parametrized XC functionals.[6] The TZ2P triple zeta basis set with two polarization functions was used for all atoms, with a small (optimization) or large (Charge Displacement) frozen core. A fine integration grid has been used both in the SCF iterations and in the optimization procedure in order to converge properly the geometrical parameters. Geometrical optimization and the self consistent field (SCF) iterations have been performed including explicitly the solvent, using conductor like screening model (COSMO) as implemented in ADF (solvent=benzene).[7]

---

(4) ADF 2009.01, SCM, Theoretical Chemistry, Vrije Universiteit, Amsterdam, The Netherlands, http://www.scm.com, E. J. Baerends, J. Autschbach, A. Bérces, F. M. Bickelhaupt, C. Bo, P. M. Boerrigter, L. Cavallo, D. P. Chong, L. Deng, R. M. Dickson, D. E. Ellis, M. van Faassen, L. Fan, T. H. Fischer, C. Fonseca Guerra, S. J. A. van Gisbergen, A. W. Götz, J. A. Groeneveld, O. V. Gritsenko, M. Grüning, F. E. Harris, P. van den Hoek, C. R. Jacob, H. Jacobsen, L. Jensen, G. van Kessel, F. Kootstra, M. V. Krykunov, E. van Lenthe, D. A. McCormack, A. Michalak, J. Neugebauer, V. P. Nicu, V. P. Osinga, S. Patchkovskii, P. H. T. Philipsen, D. Post, C. C. Pye, W. Ravenek, J. I. Rodriguez, P. Ros, P. R. T. Schipper, G. Schreckenbach, J. G. Snijders, M. Solà, M. Swart, D. Swerhone, G. te Velde, P. Vernooijs, L. Versluis, L. Visscher, O. Visser, F. Wang, T. A. Wesolowski, E. M. van Wezenbeek, G. Wiesenekker, S. K. Wolff, T. K. Woo, A. L. Yakovlev and T. Ziegler.

(5) Perdew, J. P. *Phys. Rev. B* **1986**, *33*, 8822; Treutler, O.; Ahlrichs, R. *J. Chem. Phys.* **1995**, *102*, 346.

(6) Grimme, S.; Antony, J.; Ehrlich, S.; Krieg, H. *J. Chem. Phys.* **2010**, *132*, 154104.

(7) Pye, C.C.; Ziegler, T. *Theor. Chem. Acc.*, 1999, **101**, 396.

CD Analysis relies on the CD function

$$\Delta q(z) = \int_{-\infty}^{+\infty} dx \int_{-\infty}^{+\infty} dy \int_{-\infty}^{z} dz' \Delta\rho(x, y, z')$$

where $\Delta\rho$ is the difference between the electron density of the adduct and those of its non-interacting fragments placed in the same position as they occupy in the adduct. In the present case the fragments correspond to the phosphine and the borate molecules. Δq gives a quantitative evaluation of the electronic density that moves across the plane perpendicular to the axis between the phosphorous and boron nuclei (Fig. S25-S36). Charge accumulates where the slope of $\Delta\rho$ is positive and decreases where it is negative. As boundary region between the two fragments, we chose the *z* coordinate where the two fragments show the same value of electronic density, with an error band of about 10% of the distance between phosphorous and boron atoms (grey region in the following figures).

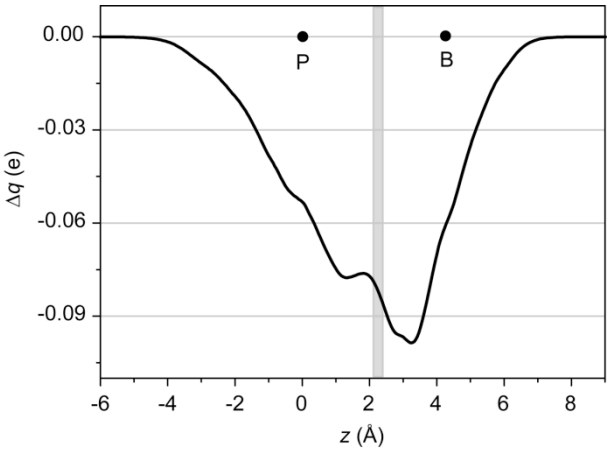

Figure S25. Charge Displacement curve for the complex **2**/B(C_6F_5)$_3$_**a** (relaxed geometry, P-B distance 4.30 Å). The black dots represents the z coordinate of the atoms. The vertical grey band identifies a suitable boundary between the phosphine and the borane. Being negative in all the regions, Δq indicates a net flow of charge between the two fragments, from the phosphine to the borane.

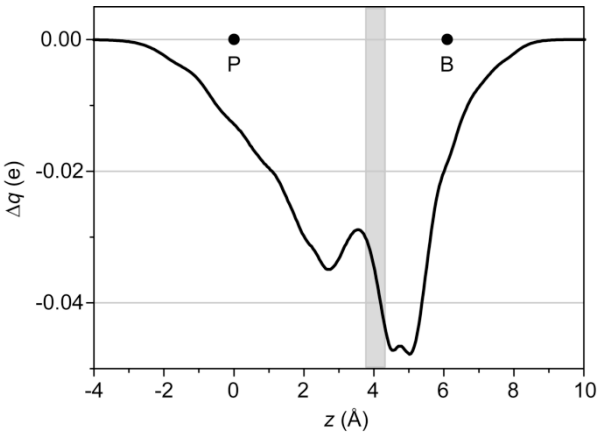

Figure S26. Charge Displacement curve for the complex **2**/B(C_6F_5)$_3$_**b** (relaxed geometry, P-B distance 6.09 Å). The black dots represents the z coordinate of the atoms. The vertical grey band identifies a suitable boundary between the phosphine and the borane.

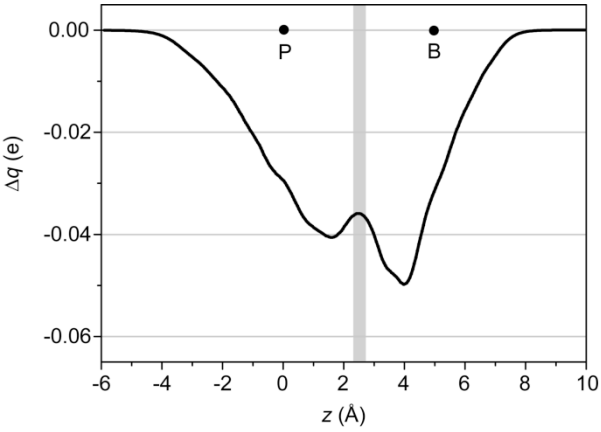

Figure S27. Charge Displacement curve for the complex **2**/B(C_6F_5)$_3$_**a** (P-B distance = 5.00 Å). The black dots represents the z coordinate of the atoms. The vertical grey band identifies a suitable boundary between the phosphine and the borane.

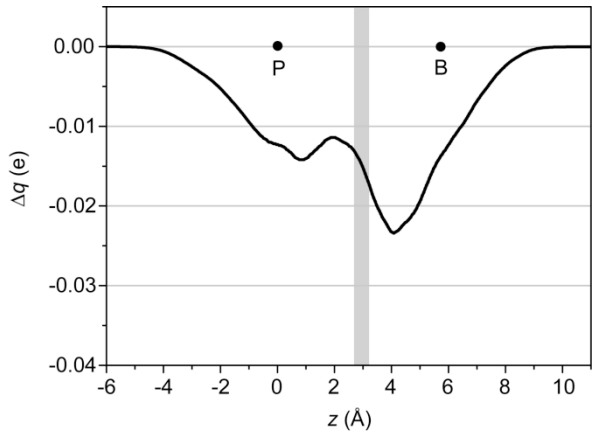

Figure S28. Charge Displacement curve for the complex **2**/B(C_6F_5)$_3$_**a** (P-B distance = 5.74 Å). The black dots represents the z coordinate of the atoms. The vertical grey band identifies a suitable boundary between the phosphine and the borane.

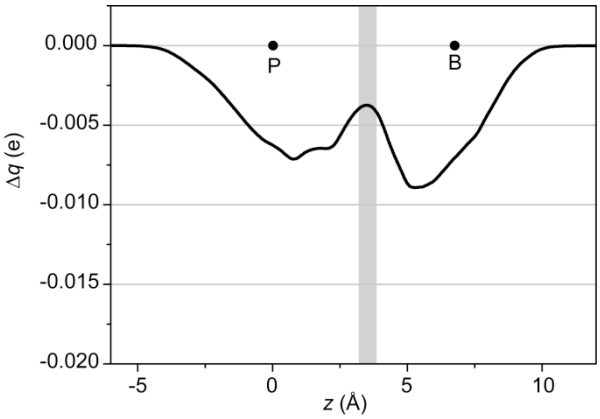

Figure S29. Charge Displacement curve for the complex **2**/B(C_6F_5)$_3$_**a** (P-B distance = 6.74 Å). The black dots represents the z coordinate of the atoms. The vertical grey band identifies a suitable boundary between the phosphine and the borane.

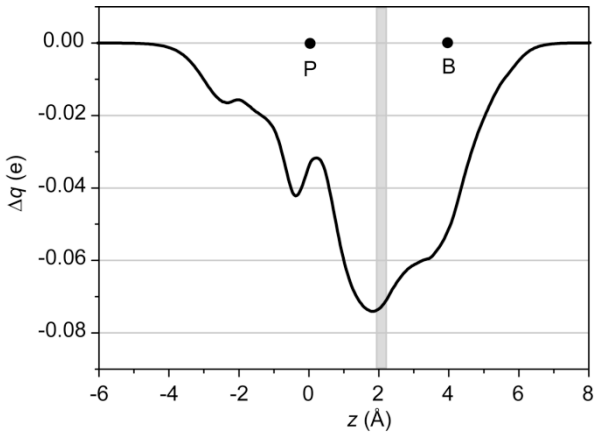

Figure S30. Charge Displacement curve for the complex **1**/B(C_6F_5)$_3$ (relaxed geometry, P-B distance = 3.90 Å). The black dots represents the z coordinate of the atoms. The vertical grey band identifies a suitable boundary between the phosphine and the borane.

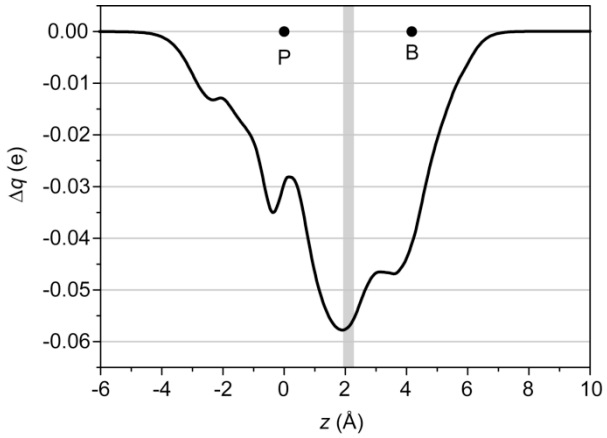

Figure S31. Charge Displacement curve for the complex **1**/B(C_6F_5)$_3$ (P-B distance = 4.16 Å). The black dots represents the z coordinate of the atoms. The vertical grey band identifies a suitable boundary between the phosphine and the borane.

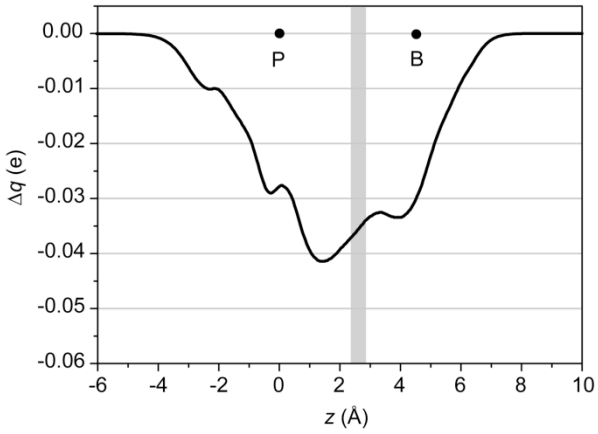

Figure S32. Charge Displacement curve for the complex **1**/B(C_6F_5)$_3$ (P-B distance = 4.56 Å). The black dots represents the z coordinate of the atoms. The vertical grey band identifies a suitable boundary between the phosphine and the borane.

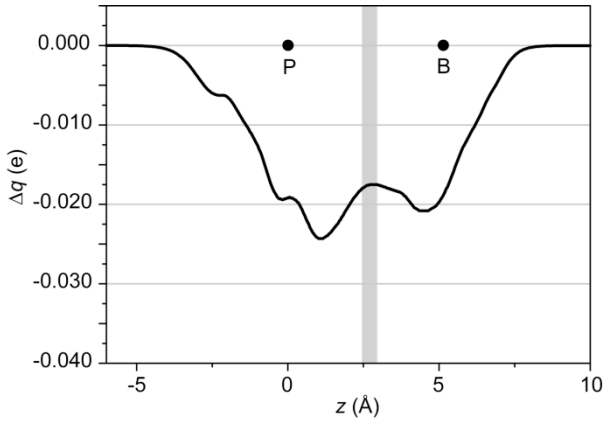

Figure S33. Charge Displacement curve for the complex **1**/B(C_6F_5)$_3$ (P-B distance = 5.16 Å). The black dots represents the z coordinate of the atoms. The vertical grey band identifies a suitable boundary between the phosphine and the borane.

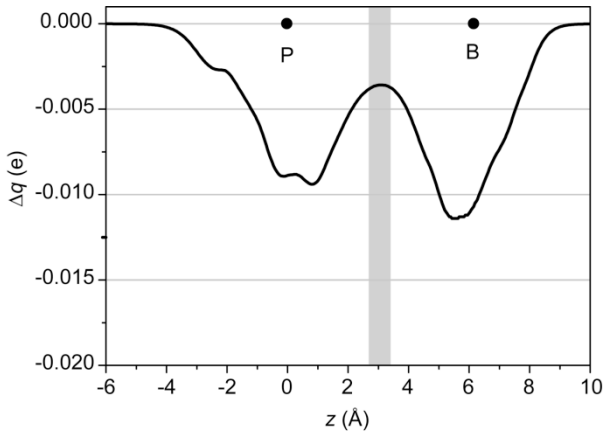

Figure S34. Charge Displacement curve for the complex **1**/B(C_6F_5)$_3$ (P-B distance = 6.16 Å). The black dots represents the z coordinate of the atoms. The vertical grey band identifies a suitable boundary between the phosphine and the borane.

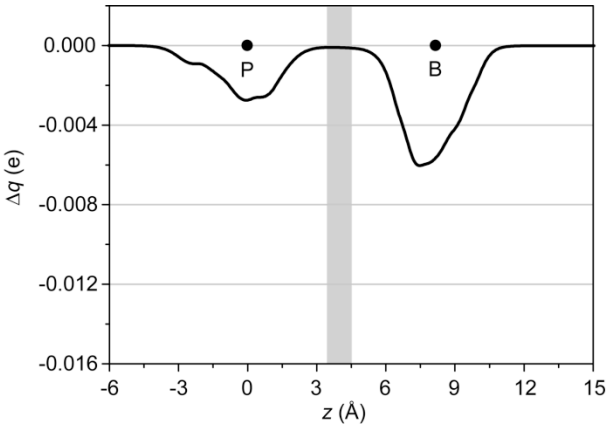

Figure S35. Charge Displacement curve for the complex **1**/B(C_6F_5)$_3$ (P-B distance = 8.16 Å). The black dots represents the z coordinate of the atoms. The vertical grey band identifies a suitable boundary between the phosphine and the borane.

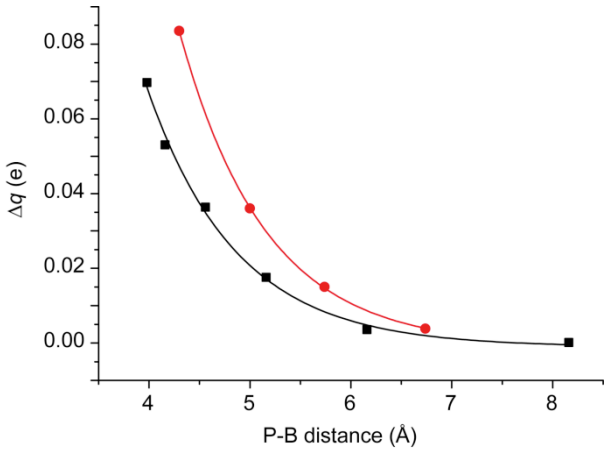

Figure S36. Trend of Δq with the P-B distance for **2**/B(C_6F_5)$_3$_**a** (red circles) and **1**/B(C_6F_5)$_3$ (black squares). The trends have been fitted with an exponential function and the equations are Δq = 13*exp(-x/0.85) – 0.0008 (R^2 = 0.9999, red line) and Δq = 6*exp(-x/0.88) – 0.001 (R^2 = 0.9947, black line).

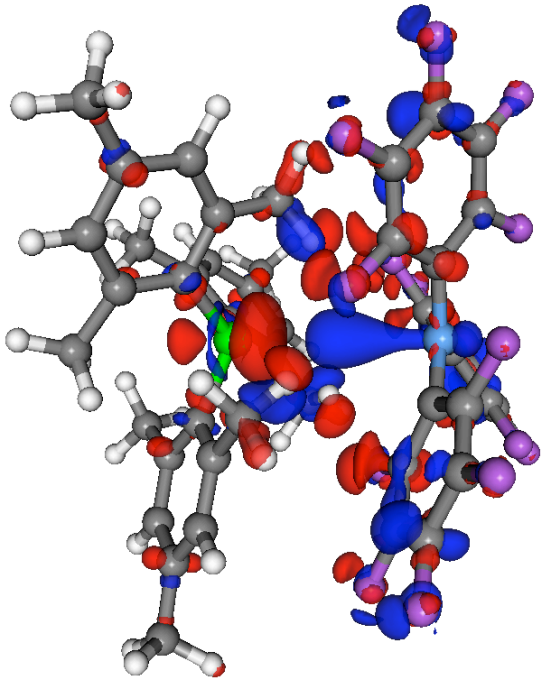

Figure S37. Three dimensional plot of electron density difference for **2**/B(C_6F_5)$_3$_**a**. Red isosurfaces identify where the electron charge is depleted, blue ones where electron charge is accumulated. Density value at the isosurface is ±0.0004 e/(u.a.)^2

The relative NOE contacts have been simulated on the basis of the DFT-optimized structures **2**/B(C_6F_5)$_3$_**a** or **2**/B(C_6F_5)$_3$_**b**, considering them as the only configuration present in solution. In particular, all the distances between magnetically equivalent proton and fluorine atoms have been averaged out on either r^{-3} and r^{-6}. The two values take into account the two possible dynamic scenarios, with the internal motions faster or slower than the overall tumbling,[8] respectively.

Table S1. Predicted NOE relative signals starting from **2**/B(C_6F_5)$_3$_**a** and considering the internal dynamics faster than the overall tumbling of the FLP ($< r^{-3} >$)

	***ortho*-CH_3**	***meta*-H**	***para*-CH_3**
***ortho*-F**	1.0	0.2	0.1
***meta*-F**	0.2	0.4	0.1
***para*-F**	0.2	0.3	0.1

Table S2. Predicted NOE relative signals starting from **2**/B(C_6F_5)$_3$_**a** and considering the internal dynamics comparable to or slower than the overall tumbling of the FLP ($< r^{-6} >$)

	***ortho*-CH_3**	***meta*-H**	***para*-CH_3**
***ortho*-F**	1.0	0.1	0.0
***meta*-F**	0.1	0.5	0.1
***para*-F**	0.2	0.3	0.0

Table S3. Predicted NOE relative signals starting from **2**/B(C_6F_5)$_3$_**b** and considering the internal dynamics faster than the overall tumbling of the FLP ($< r^{-3} >$)

	***ortho*-CH_3**	***meta*-H**	***para*-CH_3**
***ortho*-F**	1.0	0.4	0.1
***meta*-F**	0.2	0.8	0.4
***para*-F**	0.2	0.5	0.2

(8) Neuhaus, D.; Williamson, M. *The nuclear Overhauser effect in structural and conformational analysis*, VCH Publishers, Inc., **1989**.

Table S4. Predicted NOE relative signals starting from **2**/$B(C_6F_5)_3$_**b** and considering the internal dynamics comparable to or slower than the overall tumbling of the FLP ($< r^{-6} >$)

	***ortho*-CH_3**	***meta*-H**	***para*-CH_3**
***ortho*-F**	0.7	0.2	0.0
***meta*-F**	0.1	1.0	0.4
***para*-F**	0.1	0.3	0.1

XYZ Coordinates

2/$B(C_6F_5)_3$_**a**
E = -13702.62 kcal/mol

C	-1.759001	-4.086866	4.333232
C	-2.406509	-3.042707	3.675507
C	-1.833262	-1.776558	3.679573
C	-0.611706	-1.480983	4.311415
C	-0.011745	-2.565724	4.975182
C	-0.555390	-3.845738	4.993718
B	0.025441	-0.049084	4.311264
C	-0.900150	1.212968	4.388339
C	-0.576444	2.443165	3.787857
C	-1.390529	3.567433	3.857994
C	-2.592349	3.496856	4.560182
C	-2.956067	2.306733	5.187951
C	-2.115711	1.202378	5.095598
F	-1.031576	4.719749	3.271100
F	0.566365	2.586190	3.095661
F	-3.388869	4.569700	4.640792
F	-4.103101	2.244756	5.884362
F	-2.514115	0.100458	5.762356
F	-2.514222	-0.820419	3.025792
F	1.131980	-2.399263	5.669313
F	-3.575818	-3.271245	3.058005
F	0.057169	-4.846251	5.648261
F	-2.295799	-5.313288	4.339752
C	1.583121	0.115999	4.340051
C	2.212090	1.157053	5.047020
C	3.591715	1.328051	5.089908
C	4.413446	0.429353	4.411860
C	3.844457	-0.633436	3.712736
C	2.461806	-0.772330	3.692611
F	5.743447	0.578326	4.443172
F	4.140419	2.337202	5.786382
F	4.637790	-1.512555	3.081502
F	1.487024	2.037982	5.764896
F	1.987386	-1.820956	2.999990
C	-0.853568	4.544663	-0.833029
C	0.131733	3.893673	-1.575904

C	0.384821	2.520404	-1.461907
C	-0.366508	1.763365	-0.530640
C	-1.420382	2.398850	0.181498
C	-1.641521	3.765779	0.018466
P	0.016791	0.054811	0.016978
C	-1.260616	-1.113509	-0.591957
C	-1.287809	-2.371063	0.070538
C	-2.356788	-3.242090	-0.138214
C	-3.417371	-2.918766	-0.987860
C	-3.341470	-1.711778	-1.683995
C	-2.282659	-0.808681	-1.524053
C	-0.152239	-2.810895	0.948419
C	-2.269831	0.404493	-2.418494
C	-4.599506	-3.840461	-1.143092
C	1.403883	1.925546	-2.399681
C	-2.344079	1.610535	1.064245
C	-1.063327	6.033120	-0.941544
C	1.678541	-0.447150	-0.576078
C	1.944035	-1.456114	-1.532689
C	3.258161	-1.922443	-1.674635
C	4.325555	-1.409866	-0.937927
C	4.058673	-0.352942	-0.062869
C	2.767562	0.135644	0.129613
C	0.906568	-2.020631	-2.469158
C	2.561689	1.313281	1.037975
C	5.719324	-1.965367	-1.080237
H	3.450787	-2.707844	-2.408817
H	4.880313	0.108794	0.489492
H	-2.357367	-4.203040	0.381075
H	-4.127389	-1.463719	-2.400862
H	0.721063	4.469512	-2.292937
H	-2.456826	4.233733	0.574722
H	0.743317	-3.048705	0.355599
H	0.149677	-2.008610	1.633562
H	-0.418998	-3.702406	1.528590
H	-2.597377	1.318157	-1.902973
H	-1.264247	0.611907	-2.803509
H	-2.939781	0.242866	-3.271709
H	-4.298466	-4.893934	-1.079236
H	-5.336798	-3.663955	-0.345064
H	-5.108691	-3.682917	-2.101886
H	-3.010175	0.965911	0.471919
H	-1.779776	0.933988	1.717969
H	-2.970517	2.270067	1.676633
H	2.371806	1.737534	-1.914207
H	1.069082	0.961545	-2.801306
H	1.577828	2.608473	-3.240087
H	-2.129410	6.292213	-0.904292
H	-0.572988	6.556637	-0.106758
H	-0.642830	6.430941	-1.873209

H	2.323305	2.222992	0.467608
H	1.707902	1.149159	1.707117
H	3.458376	1.516060	1.635894
H	0.229770	-1.241181	-2.839181
H	1.399917	-2.487340	-3.330438
H	0.270798	-2.781090	-1.994382
H	6.462623	-1.163038	-1.180663
H	5.996886	-2.553135	-0.192447
H	5.801774	-2.622562	-1.954173

2/$B(C_6F_5)_3$_**b**

E =-13700.79 kcal/mol

C	-2.682662	-3.580074	4.195401
C	-3.060575	-2.394777	3.566445
C	-2.209251	-1.296659	3.613233
C	-0.967183	-1.312289	4.274124
C	-0.644902	-2.525574	4.908628
C	-1.467929	-3.645866	4.876915
B	-0.018310	-0.069428	4.329652
C	-0.622003	1.372763	4.386471
C	0.001678	2.485917	3.793879
C	-0.527349	3.770627	3.844108
C	-1.733518	3.988353	4.508373
C	-2.385763	2.922118	5.126517
C	-1.824928	1.651471	5.059511
F	0.114030	4.806100	3.281253
F	1.162896	2.348748	3.133365
F	-2.254879	5.218428	4.564896
F	-3.534793	3.135736	5.786331
F	-2.486521	0.676215	5.712988
F	-2.634211	-0.191356	2.980271
F	0.492565	-2.646442	5.620688
F	-4.247032	-2.325214	2.944414
F	-1.115324	-4.779682	5.502490
F	-3.490114	-4.645280	4.158031
C	1.532784	-0.268180	4.367386
C	2.375219	0.586579	5.100945
C	3.756437	0.435339	5.155208
C	4.354827	-0.614976	4.460276
C	3.564036	-1.502788	3.732245
C	2.186595	-1.318129	3.696719
F	5.681060	-0.779775	4.503598
F	4.515283	1.276455	5.874887
F	4.141432	-2.532562	3.094815
F	1.861073	1.597339	5.828656
F	1.488352	-2.206855	2.971732
C	-4.017482	-1.861055	-0.780012
C	-2.882654	-2.275416	-0.084086
C	-1.627102	-1.680651	-0.260164
C	-1.488554	-0.637394	-1.206346

C	-2.636432	-0.200919	-1.923092
C	-3.871127	-0.806565	-1.686198
P	0.081578	0.135909	-1.758566
C	0.202158	1.845336	-1.101872
C	1.147475	2.663403	-1.777634
C	1.247340	4.017620	-1.452661
C	0.420833	4.612589	-0.496057
C	-0.499878	3.794991	0.159804
C	-0.619258	2.425963	-0.105637
C	2.080536	2.093835	-2.814337
C	-1.579007	1.637924	0.741666
C	0.506221	6.087670	-0.197786
C	-0.507911	-2.152719	0.625380
C	-2.560368	0.933884	-2.910986
C	-5.351918	-2.531591	-0.574463
C	1.508292	-0.858166	-1.171157
C	2.426813	-0.496680	-0.156429
C	3.557697	-1.295205	0.051234
C	3.805632	-2.456334	-0.680861
C	2.871941	-2.817783	-1.655771
C	1.744172	-2.040145	-1.924440
C	2.225807	0.671974	0.767612
C	0.778903	-2.501137	-2.985285
C	5.044927	-3.280717	-0.442472
H	4.262659	-1.000550	0.831525
H	3.026101	-3.732291	-2.233089
H	1.992620	4.626057	-1.970107
H	-1.145191	4.231844	0.924989
H	-2.973353	-3.086881	0.641127
H	-4.744199	-0.445196	-2.234620
H	2.807036	1.399893	-2.365574
H	1.525239	1.510430	-3.563255
H	2.636909	2.891691	-3.319642
H	-2.474362	1.318479	0.192257
H	-1.113676	0.720360	1.123331
H	-1.908547	2.241293	1.596523
H	1.535863	6.456244	-0.289474
H	-0.111740	6.665979	-0.901559
H	0.148073	6.311809	0.814476
H	-2.344035	1.890248	-2.411751
H	-1.742604	0.774009	-3.628945
H	-3.504209	1.039582	-3.458194
H	0.247225	-2.740364	0.087026
H	0.028657	-1.307389	1.074289
H	-0.904531	-2.779542	1.433759
H	-6.157901	-1.793577	-0.465007
H	-5.609225	-3.167143	-1.435035
H	-5.345797	-3.167386	0.318847
H	-0.180789	-2.815649	-2.548312
H	0.542294	-1.683693	-3.681973

H	1.191354	-3.346286	-3.548360
H	1.201153	0.699245	1.159283
H	2.918852	0.606399	1.615524
H	2.389450	1.640298	0.276641
H	4.838565	-4.353891	-0.545488
H	5.829797	-3.028257	-1.171691
H	5.455986	-3.103109	0.558718

1/$B(C_6F_5)_3$

E= -10084.86 kcal/mol

C	-3.678267	-2.429124	4.166835
C	-3.647503	-1.216540	3.479762
C	-2.486009	-0.454703	3.495520
C	-1.309614	-0.853220	4.147909
C	-1.396536	-2.073516	4.838459
C	-2.546463	-2.856706	4.860369
B	0.001144	0.001749	4.104697
C	-0.082985	1.564230	4.142590
C	0.849498	2.382435	3.487401
C	0.769637	3.769293	3.467050
C	-0.264914	4.403939	4.152708
C	-1.199871	3.639162	4.849668
C	-1.095493	2.251796	4.833042
F	1.674208	4.502516	2.796058
F	1.878607	1.836599	2.811239
F	-0.353730	5.738945	4.151481
F	-2.184408	4.248638	5.529830
F	-2.020896	1.577224	5.544775
F	-2.529829	0.709126	2.818848
F	-0.346398	-2.537332	5.545751
F	-4.736934	-0.799331	2.812327
F	-2.580406	-4.013525	5.541432
F	-4.790622	-3.172718	4.170008
C	1.396209	-0.707907	4.142224
C	2.498958	-0.176925	4.832071
C	3.750840	-0.784169	4.851226
C	3.942801	-1.977606	4.155875
C	2.874410	-2.554289	3.471059
C	1.635080	-1.926777	3.490384
F	5.141335	-2.572411	4.156970
F	4.771500	-0.238853	5.532602
F	3.053588	-3.706616	2.802999
F	2.378981	0.961511	5.544752
F	0.645322	-2.545647	2.817974
C	2.698738	-0.676003	0.294518
C	1.786700	0.183041	-0.607122
P	0.000232	-0.001184	0.121281
C	-0.733790	-1.641371	-0.604181
C	-1.934240	-2.000199	0.297171

C	2.283137	1.631439	-0.447935
C	1.979001	-0.226914	-2.075338
C	-1.054089	1.452859	-0.606220
C	-2.555798	1.157202	-0.443349
C	-0.798547	1.822888	-2.075339
C	-0.765452	2.673529	0.293201
C	0.272391	-2.794851	-0.442502
C	-1.184368	-1.605556	-2.072583
H	3.361960	1.650321	-0.671831
H	3.031074	-0.054688	-2.358898
H	3.744754	-0.550092	-0.028525
H	1.796263	2.328579	-1.138146
H	2.153877	2.000759	0.574239
H	1.352698	0.361710	-2.755237
H	0.225183	2.170732	-2.250157
H	1.767904	-1.287780	-2.247509
H	2.624714	-0.347662	1.340172
H	0.276539	3.003759	0.245826
H	2.463159	-1.743465	0.249221
H	-1.474724	2.647279	-2.358415
H	-0.996265	0.985324	-2.753870
H	-1.398378	3.515843	-0.029820
H	1.119596	-2.723136	-1.132896
H	-1.011146	2.446531	1.339481
H	-0.361468	-1.358414	-2.752853
H	0.656743	-2.865082	0.579856
H	-0.250477	-3.739186	-0.664446
H	-1.997655	-0.892674	-2.245922
H	-1.561136	-2.603281	-2.354517
H	-3.112688	2.081702	-0.665791
H	-2.917310	0.386648	-1.132647
H	-2.807745	0.860533	0.579607
H	-1.613530	-2.098752	1.343136
H	-2.740957	-1.262656	0.250131
H	-2.348113	-2.969549	-0.024600

$B(C_6F_5)_3$

E =-5175.37 kcal/mol

C	-1.852794	-3.987124	4.328067
C	-2.412253	-2.920516	3.622608
C	-1.815326	-1.666839	3.701332
C	-0.649312	-1.421804	4.444161
C	-0.117499	-2.527861	5.126675
C	-0.700992	-3.789963	5.091354
B	0.015556	-0.013723	4.504254
C	-0.869553	1.266099	4.584688
C	-0.533417	2.451599	3.910252
C	-1.317156	3.599346	3.961041
C	-2.480851	3.596450	4.731653
C	-2.851167	2.446056	5.429858

C	-2.055320	1.309364	5.336612
F	-0.970802	4.703759	3.283092
F	0.571652	2.506822	3.141284
F	-3.239732	4.693910	4.800781
F	-3.964759	2.451105	6.177634
F	-2.454002	0.231997	6.040821
F	-2.390335	-0.674655	2.993264
F	0.985341	-2.389988	5.889313
F	-3.514062	-3.116694	2.883010
F	-0.173385	-4.815193	5.776940
F	-2.420183	-5.195697	4.273656
C	1.569046	0.110183	4.484017
C	2.254451	1.048220	5.272397
C	3.640739	1.159828	5.281028
C	4.396684	0.325790	4.455653
C	3.759740	-0.613863	3.643610
C	2.372916	-0.713712	3.679816
F	5.728981	0.427751	4.441996
F	4.257564	2.055371	6.066537
F	4.489370	-1.405514	2.843331
F	1.573538	1.870624	6.094940
F	1.808755	-1.628500	2.866384

$P(tBu)_3$

E= -4896.91 kcal/mol

C	-3.120283	1.068100	-3.018885
C	-3.621412	-0.138605	-2.203408
P	-3.181794	0.146022	-0.338722
C	-4.246899	-1.106959	0.684585
C	-3.603898	-1.181538	2.087972
C	-5.095129	-0.390725	-2.555779
C	-2.766748	-1.336891	-2.674754
C	-3.809938	1.919630	0.120693
C	-3.850696	2.046563	1.655188
C	-5.168274	2.361446	-0.444439
C	-2.713638	2.904624	-0.344484
C	-4.072991	-2.512354	0.078929
C	-5.748524	-0.815131	0.824314
H	-3.170493	0.812310	-4.089588
H	-5.194429	-0.500779	-3.649291
H	-2.866277	-1.438436	-3.767969
H	-3.729347	1.966051	-2.868646
H	-2.074459	1.308639	-2.783016
H	-5.743491	0.436719	-2.244999
H	-5.166035	2.412540	-1.539626
H	-5.478986	-1.312309	-2.102605
H	-1.705100	-1.175725	-2.441502
H	-2.629532	2.973126	-1.432628
H	-3.071361	-2.286323	-2.225690
H	-5.405723	3.372922	-0.072582

H	-5.982337	1.694903	-0.136848
H	-2.954021	3.911370	0.034976
H	-4.596312	-2.632353	-0.875885
H	-1.731943	2.614040	0.054703
H	-6.252340	-0.758303	-0.147556
H	-3.012716	-2.760776	-0.067198
H	-4.495041	-3.250360	0.780067
H	-5.941726	0.120170	1.362714
H	-6.225095	-1.626329	1.401090
H	-3.993290	3.107922	1.915079
H	-4.676133	1.485894	2.107021
H	-2.908285	1.715637	2.113034
H	-2.528946	-1.397442	2.014665
H	-3.725468	-0.261788	2.666842
H	-4.079865	-1.997793	2.655876

$P(Mes)_3$

E= 8513.86 kcal/mol

P	-0.074884	-0.158913	4.518679
C	-0.227988	-0.436992	2.712182
C	-0.213569	-0.467756	-0.127027
C	-0.538211	0.736225	1.972493
C	0.060183	-1.634274	2.013248
C	0.070607	-1.615990	0.613616
C	-0.534616	0.695067	0.577173
H	0.290691	-2.546674	0.085809
H	-0.785532	1.604092	0.026038
C	-1.738126	-0.039690	5.282546
C	-4.187988	0.588137	6.573033
C	-2.971135	-0.395261	4.683989
C	-1.746272	0.605762	6.548597
C	-2.962683	0.895919	7.168922
C	-4.162838	-0.062744	5.338717
H	-2.948751	1.383223	8.146355
H	-5.107516	-0.345396	4.868740
C	0.877976	-1.522766	5.290540
C	2.647061	-3.293181	6.631124
C	2.283369	-1.421402	5.105572
C	0.366653	-2.540610	6.131499
C	1.263711	-3.391539	6.787698
C	3.133517	-2.309162	5.767243
H	0.857052	-4.175077	7.431038
H	4.210115	-2.222500	5.604578
C	2.883139	-0.390240	4.184393
H	3.977522	-0.402641	4.245758
H	2.519346	0.616883	4.435156
H	2.595366	-0.566175	3.137508
C	-0.901047	2.027061	2.660714
H	-0.134265	2.305910	3.398188
H	-1.843483	1.936463	3.220470

H	-1.011512	2.839053	1.932657
C	-0.465041	0.962787	7.257522
H	0.106610	0.065657	7.536984
H	-0.670805	1.535838	8.169045
H	0.193317	1.551687	6.602326
C	-1.104767	-2.801141	6.323079
H	-1.580998	-2.055080	6.974184
H	-1.255835	-3.789955	6.772714
H	-1.647872	-2.768080	5.370795
C	0.305833	-2.956507	2.692152
H	1.302017	-3.012521	3.152366
H	0.221229	-3.773435	1.965365
H	-0.414983	-3.135916	3.499069
C	-3.079143	-1.167798	3.395146
H	-2.370787	-2.004630	3.365619
H	-2.858548	-0.547638	2.515343
H	-4.093325	-1.569466	3.281730
C	3.583785	-4.203625	7.384403
H	4.512183	-4.375572	6.825526
H	3.118439	-5.175872	7.589827
H	3.861815	-3.762423	8.353811
C	-5.492205	0.964117	7.229890
H	-5.402154	0.975963	8.323317
H	-6.294153	0.266965	6.956270
H	-5.811667	1.969820	6.916504
C	-0.155407	-0.477409	-1.633789
H	0.853353	-0.214636	-1.987423
H	-0.853177	0.250080	-2.067054
H	-0.394680	-1.469241	-2.037560